Numerical Simulation of Macroscopic Mixing in a Rushton Impeller Stirred Tank

WANG Zheng(王 正)[1,2], MAO Zai-sha(毛在砂)[1], SHEN Xian-qian(沈湘黔)[3]

(*1. Institute of Process Engineering, Chinese Academy of Sciences, Beijing 100080, China;*
2. Graduate University of Chinese Academy of Sciences, Beijing 100049, China;
3. Changsha Research Institute of Mining and Metallurgy, Changsha, Hunan 410012, China)

Abstract: The macroscopic mixing in a stirred tank with different tracer injection locations, impeller speeds and impeller positions is simulated numerically by solving the transport equation of the tracer based on the whole flow field in the baffled tank with a Rushton disk turbine numerically resolved using the improved inner–outer iterative procedure. Predicted mixing time is compared well with the literature correlations. The predicted residence time distribution of the stirred tank is very close to the present experimental results. The effect of the installation of a draft tube on the mixing time and residence time distributions is addressed.

Key words: macroscopic mixing; stirred tank; residence time distribution; mixing time; numerical simulation
CLC No.: TQ027.2 **Document Code:** A **Article ID:** 1009−606X(2006)06−0857−07

1 INTRODUCTION

Mixing in stirred tank reactors occurs as a result of the medium motion at three levels: molecular, eddy and bulk motions. Usually, the bulk motion is superimposed on either molecular or eddy diffusion or both. Mixing on the vessel scale is called as macroscopic mixing, which is the focus deliberated in this work. Since the mixing of reactants with one another in stirred tanks shows substantial influence on productivity, conversion rate and selectivity of chemical reactors, the study on fluid flow and mixing in stirred tanks is now being intensively conducted via experimental investigation (usually tracer experiments) and computational fluid dynamics (CFD) based on mathematical modeling.

In a tracer experiment, certain amount of tracer (usually in the form of a pulse) is injected at some location in a reactor and the tracer concentration as a function of time is monitored to obtain the mixing time, which is defined as the time required to achieve a certain degree of uniformity of tracer concentration to characterize the mixing process. The tracer used can be thermal disturbance, chemical species, or other substances that track the bulk fluid flow, and the measurement technique is then selected correspondingly, such as visual observation[1], conductivity technique[2–4], laser-induced fluorescence technique[5] and liquid-crystal thermography[6]. Some empirical correlations merely correlate the experimental data with the design and operating parameters[4,7,8], and some semi-empirical models such as circulation models[9], dispersion models[2,10] and network of zones models[11] were also reported in the recent literature.

The mathematical modeling and numerical simulation of mixing process present a flexible predicting tool for mixing time under diversified tank configurations and operating conditions for the macroscopic and microscopic mixing in non-reacting and reacting systems.

Use of CFD modeling for the mixing studies was explored for the first time by Ranade et al.[11]. The CFD software Fluent was used to predict the flow pattern and mixing process in a stirred tank equipped with dual-Rushton turbines by Jaworski et al.[12]. Zhou et al.[13] used the commercial code CFX to simulate the mixing process of a single Rushton turbine in a stirred tank and obtained that the mixing time highly relied on the flow field, the feeding and detecting positions.

The other index to characterize the macroscopic mixing in chemical reactors is the residence time distribution (RTD), which is synonymic with the exit age distribution density function $E(t)$[14]. RTD can also be approached either experimentally or numerically, and the latter requires solving both the turbulent flow and the mass transport in a reactor[15,16].

The draft tube is usually used to provide gross

Received date: 2005−09−13; **Accepted date:** 2005−12−06
Foundation item: Supported by the National Natural Science Foundation of China (No.20236050; 50134020); The National Basic Research Priorities Program (973) (No.2004CB217604)
Biography: WANG Zheng(1977−), male, native of Wuwei County, Anhui Province, major in chemical technology; MAO Zai-sha, corresponding author, E-mail: zsmao@home.ipe.ac.cn.

circulation and improve suspending solids in the agitated reactor especially as industrial crystallizer[17]. Its installation also improves the property uniformity of precipitating products. So far the effect of the draft tube in a stirred tank has not been clarified from the point of view of macroscopic mixing. In this work, the mixing time and RTD of stirred tanks are numerically approached by solving the transport equation of the tracer based on the numerically resolved flow field in a baffled tank with a Rushton disk turbine using the improved inner–outer iterative procedure. Predicted mixing time and the residence time distribution are compared with the experimental results. The effect of the presence of a draft tube on mixing time and RTD is also analyzed.

2 EXPERIMENTAL

2.1 Experimental Stirred Tank

The experiment on mixing time in the flat-bottomed cylindrical stirred tank with the diameter of T=0.54 m without draft tube, equipped with four baffles (width equal to T/10) equally spaced around the perimeter[18] is numerically simulated. The working fluid is water, and the liquid height T is equal to the diameter. The tank is stirred with a standard Rushton turbine whose diameter is one-third of the tank diameter. A schematic diagram of the tank and impeller is shown in Fig.1, and $P1$, $P2$, $P3$ are the injection points, B, C, D, E, F, G are the detector points. The coordinates of these positions are listed in Tables 1 and 2 (with the center of the tank bottom as the origin of the cylindrical coordinate system).

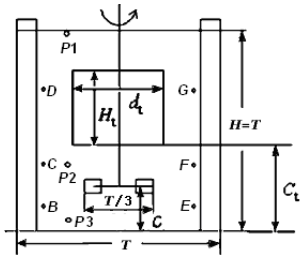

Fig.1 Sketch of a baffled stirred tank

Table 1 Positions of injection points

Position	r (m)	θ (rad)	z (m)
$P1$	0.10	π/4	0.534
$P2$	0.15	π/4	0.180
$P3$	0.15	π/4	0.060

Table 2 Positions of detectors

Position	r (m)	θ (rad)	z (m)
B	0.225	π/4	0.090
C	0.225	π/4	0.180
D	0.225	π/4	0.360
E	0.225	5π/4	0.090
F	0.225	5π/4	0.180
G	0.225	5π/4	0.360

2.2 RTD Measurement

The stirred tank for the present RTD study is a flat-bottomed cylindrical vessel (T=0.154 m, with/without draft tube) geometrically similar to that in Fig.1. The experimental apparatus is shown in Fig.2. The residence time distribution was determined experimentally by injecting 1 mL of 5 mol/L sodium chloride solution into the tank being operated with a constant inlet flow rate and the impeller speed was set between 200 and 400 r/min. The feeding tube was located at the free surface, mid-way between two neighboring wall baffles and roughly at r=T/4. The outlet stream conductivity was monitored with a conductometer and the signal collected into a computer right from the instant of the pulse injection until the conductivity fell to a very low level. The signal was then transformed into the tracer concentration as the function of time with a calibration curve.

The effect of the installed draft tube on the residence time distribution is also experimentally studied. The internal diameter of the draft tube used was 0.54T and 0.68T, respectively, with H_t/T=0.5, C_t/T=0.4.

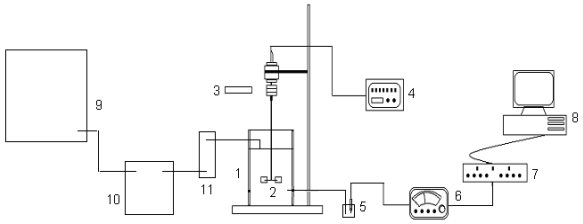

1. Stirred vessel 2. Rushton turbine 3. Laser tachometer
4. Speed controller 5. Conductivity electrode 6. Conductometer
7. Amplifier 8. Computer 9. Water tank
10. Peristaltic pump 11. Flowmeter

Fig.2 Schematic diagram of the experimental apparatus

3 MATHEMATICAL MODEL

3.1 Governing Equations

The liquid flow and tracer transport, in terms of velocity components u, v, w, turbulent kinetic energy k, viscous dissipation ε, and tracer concentration c, are described by the general partial differential equation in the cylindrical coordinate system as

$$\frac{\partial(\rho\phi)}{\partial t}+\frac{1}{r}\frac{\partial}{\partial r}(\rho ur\phi)+\frac{1}{r}\frac{\partial}{\partial\theta}(\rho v\phi)+\frac{\partial}{\partial z}(\rho w\phi)=\frac{1}{r}\frac{\partial}{\partial r}\left(r\Gamma_{\phi,\mathrm{eff}}\frac{\partial\phi}{\partial r}\right)+\frac{1}{r}\frac{\partial}{\partial\theta}\left(\frac{\Gamma_{\phi,\mathrm{eff}}}{r}\frac{\partial\phi}{\partial\theta}\right)+\frac{\partial}{\partial z}\left(\Gamma_{\phi,\mathrm{eff}}\frac{\partial\phi}{\partial z}\right)+S, \quad (1)$$

where ϕ is the dependent variable and S is the source term per volume. The eddy diffusivity was modeled using a standard k–ε model, and the action of impeller rotation was modeled using the improved inner–outer

iterative procedure. The detailed description of the governing equations and the numerical procedure has already been given by Wang et al.[19] for single phase flow. For the transport equation of the tracer concentration, the diffusion coefficient $\Gamma_{c,eff}$ is related to the turbulent viscosity μ_{eff} via a turbulent Schmidt number Sc according to $\Gamma_{c,eff}=\mu_{eff}/Sc$, in which Sc equals to 1.0 and μ_{eff} comes from the prediction of the flow field.

3.2 Prediction of Mixing Time

An in-house computer program was used to solve numerically the mathematical models for the fluid flow and the macromixing of the injected tracer on a PC computer. The flow field and mixing process in the tank are computed on a grid of 36×48×90 ($r\times\theta\times z$), which has been justified to be nearly grid-independent numerical solution[20].

The mixing time characterizing the macroscopic mixing process is defined as the time required for the concentration at certain detector point to reach the final average concentration within ±5% in this work. A zero-flux boundary condition for c is enforced at the tank wall and the liquid surface. To start the numerical simulation at t=0 s, the concentration in the cell at injection point is set to 1.0 mol/L, while the initial concentration at other cells are all set to 0 mol/L. The change of tracer concentration with time is obtained by solving the tracer transport equation based on the numerical results of the flow field (not shown here) in the baffled tank using the improved inner–outer iterative procedure. The mixing time of every detecting position is found from the time trace of tracer concentration at that point.

3.3 Prediction of Residence Time Distribution

In such simulation, the addition of tracer was still in the form of a pulse. An inlet liquid stream was fed into and an outlet stream was drawn from the tank at the same flow rate, and the tracer concentration transport equation was solved by an implicit method using the control volume formulation based on the resolved flow field in the baffled tank. The mean residence time was computed by

$$t_m=\int_0^\infty tC_{out}(t)\mathrm{d}t\Big/\int_0^\infty C_{out}(t)\mathrm{d}t\,. \tag{2}$$

The exit age distribution density function, $E(t)$, was calculated in the following manner:

$$E(t)=C_{out}(t)\Big/\int_0^\infty C_{out}(t)\mathrm{d}t\,. \tag{3}$$

The variance of the standard deviation of the RTD was calculated using

$$\sigma^2=\int_0^\infty (t-t_m)^2E(t)\mathrm{d}t\,. \tag{4}$$

4 SIMULATION RESULTS OF MIXING TIME

4.1 Effect of Injection Points on Mixing Time

Figure 3 shows the results of response curves from detectors C and D with different injection positions. The shape of response curves varies with the injection position, mainly due to dissimilar relative position between the injection and detector points. The peak of the response curves of detector C with injection at point $P2$ is much higher than those at other injection positions [in Fig.3(a)], because detector C is very close to the injection points $P2$. Although detector D is closer to the injection point $P1$, the response peak at injection point $P2$ is higher, because the tracer takes shorter time from $P2$ to reach D (with less dispersion) than that from $P1$ to D along the clockwise streamlines in the upper left corner of the tank [in Fig.3(b)]. The mixing time at different injection points $P1$, $P2$, and $P3$ (averaged between different detectors) are 16.08, 16.34, 16.20 s (N=250 r/min), respectively. So it can be concluded that

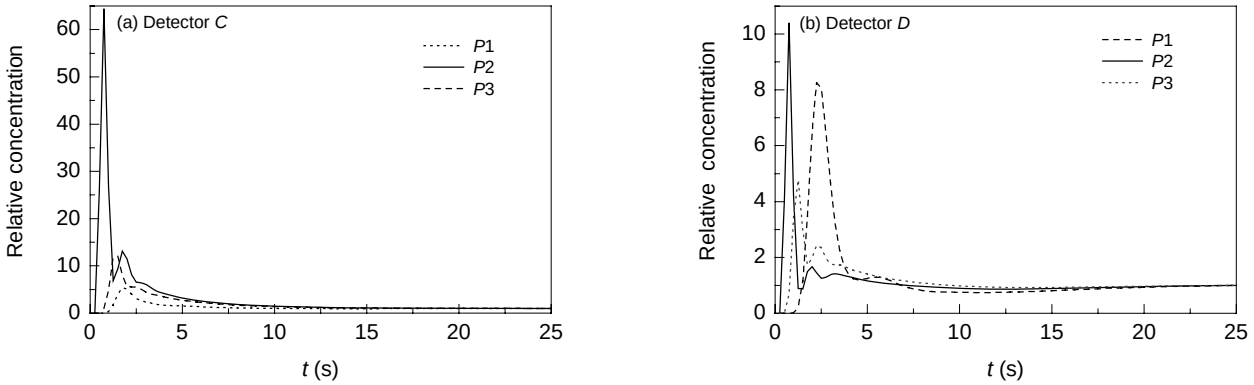

Fig.3 Tracer response from detector C and D with different injection points

the mixing time is almost independent of the location of the simulation results of Zhou et al.[13], but in good coincidence with the literature data and conclusions from other researchers[1,4].

4.2 Effect of Impeller Speed on Mixing Time

The mixing times by different detectors all decrease as the impeller speed increases. The response curves of detector *C* at different impeller speeds are shown in Fig.4.

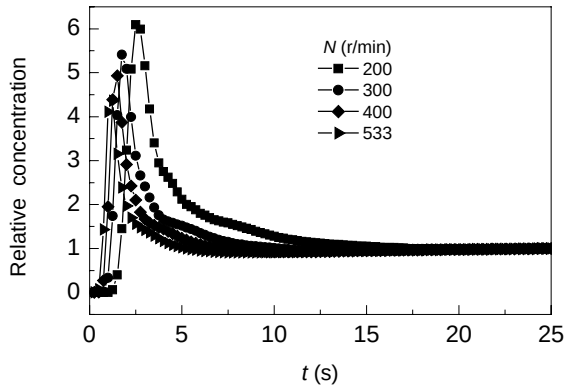

Fig.4 Tracer response from detector *C* at different impeller speeds at point *P*1

The correlation of dimensionless mixing time with the various design and operation parameters has been developed in the literature. For the stirred tank driven by disk turbine, Joshi et al.[7] proposed the following correlation of the mixing time:

$$N\theta_{\mathrm{m}} = 9.43\left(\frac{aH+T}{T}\right)(T/D_{\mathrm{d}})^{13/6}(W_{\mathrm{d}}/D_{\mathrm{d}}), \quad (5)$$

and Shiue et al.[8] suggested

$$N\theta_{\mathrm{m}}=5.01(T/D_{\mathrm{d}})^{2.4}. \quad (6)$$

The dimensionless mixing time $N\theta_{\mathrm{m}}$ will remain constant if the impeller speed remains just in the turbulent region while other design and operation parameters are held unchanged. The comparison of the dimensionless mixing time predicted by the CFD simulation with correlations[7,8] and experimental data[18] in the literature are listed in Table 3. It can be concluded that the predicted results of $N\theta_{\mathrm{m}}$ are inside the range evidenced in the literature. The discrepancy among various studies can be attributed to the difference in geometry investigated and the measurement technique employed. And the deviation of the predicted results with the experimental data may be attributed to the inaccuracy of the predicted flow pattern which was obtained by solving the Raynolds-averaged Navier–Stokes equations using the standard k–ε model.

Table 3 Comparison of $N\theta_{\mathrm{m}}$ predicted by CFD and the literature correlations

Impeller speed (r/min)	Joshi et al.[7]	Shiue et al.[8]	Experimental result[18]	Numerical prediction
200	47.5	70	52	65
250	47.5	70	–	67.1
300	47.5	70	50	67.5
400	47.5	70	–	66.6
533	47.5	70	51	66.6

4.3 Effect of Impeller Clearance on Mixing Time

Figure 5 shows the results of response curves of detector *B* at different impeller clearance *C*. The mixing time at different impeller clearance *C*=*T*/2, *T*/3, *T*/6, which is averaged over different detectors, is 13.6, 16.1 and 16.5 s (*N*=250 r/min) respectively. It suggests that the mixing time for the disk turbine increases as the impeller clearance decreases from *T*/2 to *T*/6, in agreement with Brennan and Lehrer's experimental results[1], for the overall mixing in the upper tank is weakened. It is also confirmed that the dimensionless mixing time increases when the impeller clearance decreases from Joshi's correlation[7] about the disk turbine where *a* is equal to 1 when impeller is situated centrally or equal to 1.33 if *C* is equal to *T*/3 and so on.

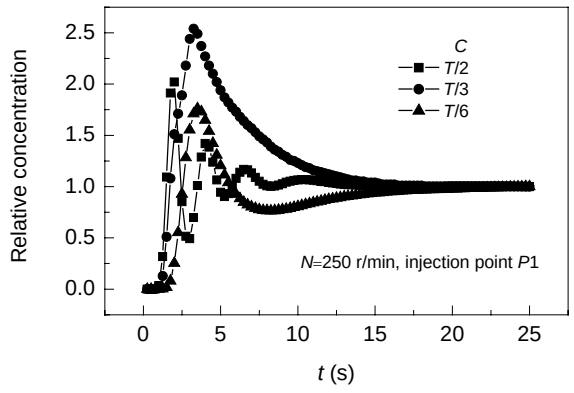

Fig.5 Tracer response from detector *B* with different impeller clearance

4.4 Effect of Draft Tube on Mixing Time

Draft tubes are very common in a number of specialized designs such as crystallizers and precipitators in which mass transfer seems to dominate the operation[21,22]. The effect of the presence of draft tube on mixing time was investigated numerically in this work. The geometric characteristics of draft tubes

are listed in Table 4. The mixing time for the cases 1~5 (averaged over six detectors) is determined from the response curves in Fig.6 to be 16.5, 16.7, 17.0, 16.3 and 17.2 s (N=250 r/min), respectively. It can be seen that the mixing time with the presence of a draft tube seems a little larger or smaller than that obtained in a configuration without draft tube. There appears to be little difference in mixing times for the standard configuration and the configuration with a draft tube, as already reported in an early study[23]. However, it is generally admitted that the presence of a draft tube promotes flow homogeneity in stirred tanks in favor of precipitation operation, because the distribution of circulation time of particles and liquid elements would become narrower.

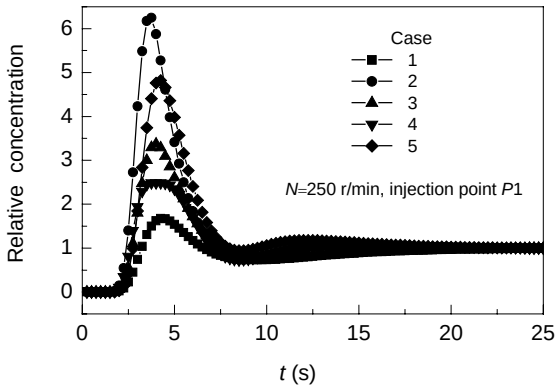

Fig.6 Tracer response from detector B with the presence of the draft tube

Table 4 Geometric dimensions of draft tube of mixing time

Case	C	d_t	C_t/T	H_t/T
1	T/6			
2	T/6	0.55D	0.44	0.44
3	T/6	0.55D	0.28	0.44
4	T/6	0.72D	0.44	0.44
5	T/6	0.72D	0.28	0.44

Table 5 Comparison of the results of the experiments and the CFD simulation

Case	Measured t_m (s)	Predicted t_m (s)	Measured σ/t_m	Predicted σ/t_m
C=T/2, N=200 r/min	810	840	0.951	0.911
C=T/2, N=300 r/min	808	844	0.956	0.925
C=T/2, N=400 r/min	821	839	0.943	0.912
C=T/6, N=200 r/min, draft tube 1	803	841	0.927	0.931
C=T/6, N=200 r/min, draft tube 2	808	832	0.932	0.928
Nominal residence time, V/Q	880			

5 EXPERIMENT AND SIMULATION ON RESIDENCE TIME DISTRIBUTION

The RTD curves obtained from the present experiment and simulation are shown in Fig.7. From the experimental RTD curve it can be seen that the outlet tracer concentration decreases in an exponential manner, following closely the ideal CSTR behavior in the rest of time, except only at the very early stage. The predicted RTD curve shows similar trends with its experimental counterparts. From Table 5, the experimental data and the simulation values at different impeller speeds show that agitation speed had little effect on the mean residence time. The experimental and simulated RTD curves with the draft tube are shown in Fig.8. Combining the hints from Figs.6~8, it seems that whether the draft tube is present or not it exerts no significant impact on the nature that a stirred tank operated in the turbulent regime is macroscopically an ideal mixed reactor, and the benefit of installed draft tube comes from the improved flow homogeneity.

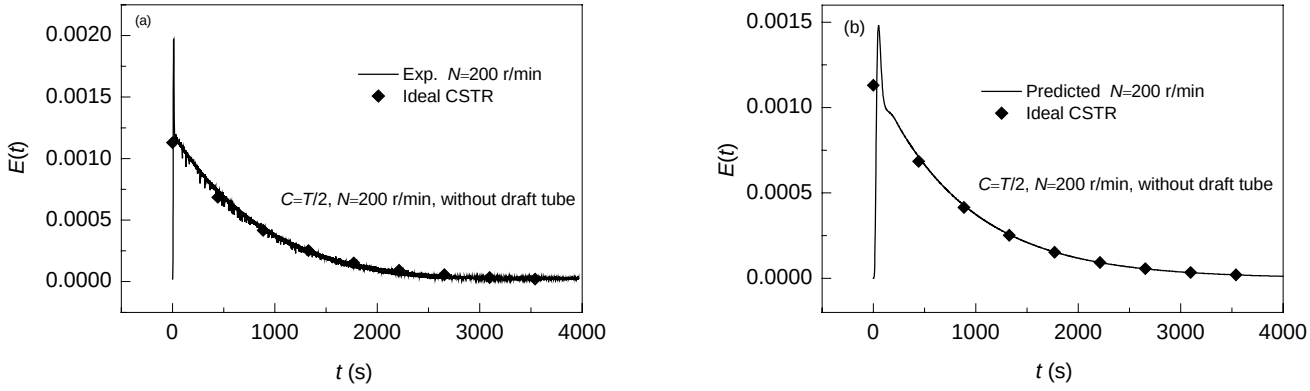

Fig.7 Comparison of the simulated $E(t)$ and experimental results

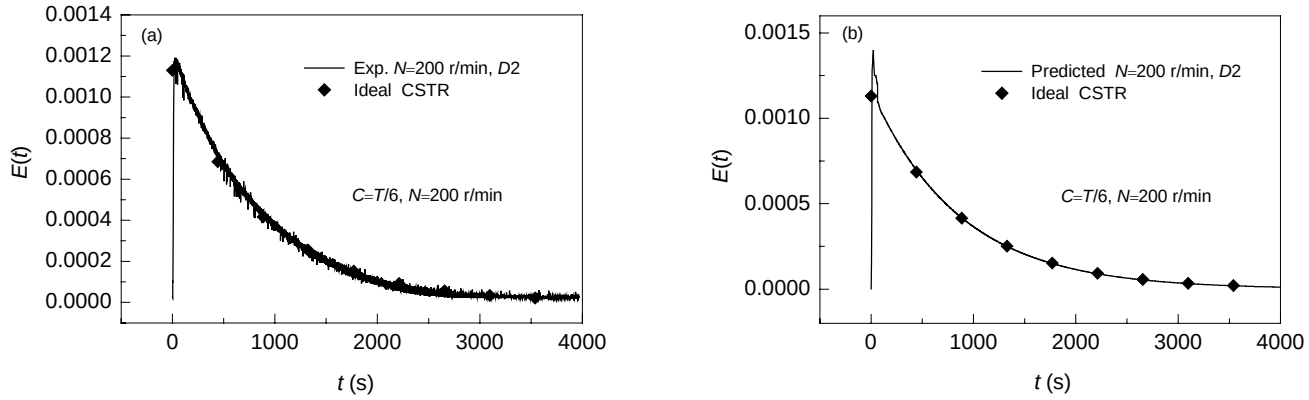

Fig.8 Comparison of $E(t)$ by CFD simulation and experimental result with draft tube 2

6 FLOW HOMOGENEITY

Although it is intuitive to conceive that the introduced draft tube improves the homogeneity of flow which may contribute to the uniformity of circulation time distribution, a quantitative index, the coefficient of variation (δ) of volume-averaged liquid velocity magnitude, is used here to quantify the effect. The average magnitude of velocity vector in the tank ($\bar{U}$), its standard deviation (σ) and δ are defined by Eqs.(7) to (9):

$$\bar{U} = \iiint \sqrt{u^2+v^2+w^2}\, r\mathrm{d}r\mathrm{d}\theta\mathrm{d}z \Big/ \iiint r\mathrm{d}r\mathrm{d}\theta\mathrm{d}z \,, \tag{7}$$

$$\sigma^2 = \iiint \left(\sqrt{u^2+v^2+w^2} - \bar{U}\right)^2 r\mathrm{d}r\mathrm{d}\theta\mathrm{d}z \Big/ \iiint r\mathrm{d}r\mathrm{d}\theta\mathrm{d}z \,, \tag{8}$$

$$\delta = \sigma/\bar{U} \,, \tag{9}$$

and calculated from the resolved flow field in the tank.

The calculated results are listed in Table 6, in which the corresponding values of the velocity magnitude in the r–z plane ($\sqrt{u^2+w^2}$) and the axial velocity component w are also shown. It is found that daft tube 1 decreases the values of $\bar{U}$ either for $\sqrt{u^2+v^2+w^2}$, $\sqrt{u^2+w^2}$ or $|w|$ as compared with the stirred tank without draft tube, but they increase when draft tube 2 with slightly large diameter is installed. It is particularly obvious that the coefficient of variation of $|w|$ for draft tube 2 (δ=0.613) is much lower than that for the stirred tank without draft tube (δ=0.895). Since the value of $|w|$ is mainly responsible for axial circulation and mixing in the tank, the smaller coefficient of variation is believed to be favorable to the product homogeneity in such a reactor.

Table 6 Effect of the draft tube on the velocity statistics from CFD simulation

Case		$\sqrt{u^2+v^2+w^2}$	$\sqrt{u^2+w^2}$	$\lvert w\rvert$
C=*T*/6, *N*=200 r/min	$\bar{U}$	0.0480	0.0438	0.0295
	σ	0.0261	0.0254	0.0264
	δ	0.5440	0.5810	0.8950
C=*T*/6, *N*=200 r/min, draft tube 1	$\bar{U}$	0.0480	0.0428	0.0287
	σ	0.0258	0.0250	0.0191
	δ	0.5380	0.5840	0.6650
C=*T*/6, *N*=200 r/min, draft tube 2	$\bar{U}$	0.0494	0.0446	0.0305
	σ	0.0253	0.0239	0.0187
	δ	0.5120	0.5360	0.6130

7 CONCLUSIONS

In the present work, the numerical prediction of the mixing time and residence time distribution of a baffled tank with a Rushton disk turbine has been explored. The predicted mixing time and mean residence time are in good agreement with the experimental measurements. The present numerical method for mixing time and residence time distribution in a stirred tank is proved reliable and applicable.

The effect of a draft tube on the mixing time and residence time distribution is found not significant, but it is suggested that the draft tube may not impact on the stirred tank performance through mixing time and residence time distribution. By analyzing the averaged velocity magnitude and its variation, it is inferred that the installation of suitable draft tube improves the flow uniformity, particularly the axial circulation and mixing,

in the stirred tank and may be favorable to the improvement of reactor performance of stirred tank.

NOTATION:

a	Ratio of the maximum length of circulation path to the height of liquid
C	Clearance of the impeller from tank bottom (m)
C_t	Distance of the draft tube to the tank bottom (m)
$C_{out}(t)$	Tracer concentration at the outlet at time t (kmol/m^3)
d_t	Draft tube diameter (m)
D_d	Impeller diameter (m)
$E(t)$	Residence time distribution (s^{-1})
H	Height of liquid in the tank (m)
H_t	Length of draft tube (m)
N	Impeller speed (r/min)
S	Source term in Eq.(1)
Sc	Turbulent Schmidt number
t_m	Mean residence time calculated from Eq.(2) (s)
T	Tank diameter (m)
$\bar{U}$	Average magnitude of velocity vector by Eq.(7) (m/s)
u	Mean radial velocity (m/s)
v	Mean tangential velocity (m/s)
V	Volume of the tank (m^3)
w	Mean axial velocity (m/s)
W_d	Impeller blade width (m)
Q	Flow rate into and out of the tank (m^3/s)
r	Radial coordinate (m)
z	Axial coordinate (m)
δ	Coefficient of variation of volume-averaged liquid velocity magnitude by Eq.(9)
ϕ	General variable
μ_{eff}	Turbulent viscosity (Pa·s)
θ	Tangential coordinate (rad)
σ	Variance of a variable to the mean

REFERENCES:

[1] Brennan D J, Lehrer I H. Impeller Mixing in Vessels Experimental Studies on the Influence of Some Parameters and Formulation of a General Mixing Time Equation [J]. Chem. Eng. Res. Des., 1976, 54(A3): 139–152.

[2] Holmes D B, Voncken R M, Dekker J A. Fluid Flow in Turbine Stirred, Baffled Tanks: I. Circulation Time [J]. Chem. Eng. Sci., 1964, 19(3): 201–208.

[3] Kramers H, Baars G M, Knoll W H. A Comparative Study on the Rate of Mixing in Stirred Tanks [J]. Chem. Eng. Sci., 1953, 2(1): 35–42.

[4] Biggs R D. Mixing Rates in Stirred Tanks [J]. AIChE J., 1963, 9(5): 636–640.

[5] Li L, Wei J. Three-dimensional Image Analysis of Mixing in Stirred Vessels [J]. AIChE J., 1999, 45(9): 1855–1865.

[6] Lee K C, Yianneskis M. A Liquid Crystal Thermographic Technique for the Measurement of Mixing Characteristics in Stirred Vessels [J]. Chem. Eng. Res. Des., 1997, 75(A8): 746–754.

[7] Joshi J B, Pandit A B, Sharma M M. Mechanically Agitated Gas–Liquid Reactors [J]. Chem. Eng. Sci., 1982, 37(6): 813–844.

[8] Shiue S J, Wong C W. Studies on Homogenization Efficiency of Various Agitators in Liquid Blending [J]. Can. J. Chem. Eng., 1984, 62(5): 602–609.

[9] McManamey W J. A Circulation Model for Batch Mixing in Agitated Baffled Vessels [J]. Chem. Eng. Res. Des., 1980, 58(4): 271–276.

[10] Voncken R M, Holmes D B, Den Hartog H W. Fluid Flow in Turbine Stirred, Baffled Tanks: II. Dispersion during Circulation [J]. Chem. Eng. Sci., 1964, 19(3): 209–213.

[11] Ranade V V, Bourne J R, Joshi J B. Fluid Mechanics and Blending in Agitated Tanks [J]. Chem. Eng. Sci., 1991, 46(8): 1883–1893.

[12] Jaworski Z, Bujalski W, Otomo N, et al. CFD Study of Homogenization with Dual Rushton Turbines—Comparison with Experimental Results [J]. Chem. Eng. Res. Des., 2000, 78(4): 327–333.

[13] Zhou G Z, Wang Y C, Shi L T. CFD Study of Mixing Process in Stirred Tank [J]. J. Chem. Ind. Eng., 2003, 54(7): 886–890 (in Chinese).

[14] Levenspiel O. Chemical Reaction Engineering, 3rd Ed. [M]. New York: John Wiley & Sons, 1999. 257–328.

[15] Patwardhan A W. Prediction of Residence Time Distribution of Stirred Reactors [J]. Ind. Eng. Chem. Res., 2001, 40(24): 5686–5695.

[16] Choi B S, Wan B, Philyaw S, et al. Residence Time Distribution in a Stirred Tank: Comparison of CFD Predictions with Experiment [J]. Ind. Eng. Chem. Res., 2004, 43(20): 6548–6556.

[17] Jones A G. Crystallization Process Systems [M]. Oxford: Butterworth-Heinemann Press, 2002. 63–65.

[18] Lunden M, Stenberg O, Andersson B. Evaluation of a Method for Measuring Mixing Time Using Numerical Simulation and Experimental Data [J]. Chem. Eng. Commun., 1995, 139(1): 115–136.

[19] Wang W J, Mao Z S. Numerical Simulation of the Whole Field in a Stirred Tank with a Rushton Turbine Using the Improved Inner–Outer Iterative Approaches [J]. Chinese J. Process Eng., 2002, 2(3): 193–198 (in Chinese).

[20] Wang W J, Mao Z S. Numerical Simulation of Gas–Liquid Flow in a Stirred Tank with a Rushton Turbine [J]. Chinese J. Chem. Eng., 2002, 10(4): 385–395.

[21] Tanaka M, Izumi T. Application of Stirred Tank Reactor Equipped with Draft Tube to Suspension Polymerization of Styrene [J]. J. Chem. Eng. Jpn., 1984, 18(4): 354–358.

[22] Penicot P, Muhr H, Plasari E, et al. Influence of the Internal Crystallizer Geometry and the Operational Conditions on the Solid Product Quality [J]. Chem. Eng. Technol., 1998, 21(6): 507–514.

[23] Tatterson G B. The Effect of Draft Tubes on Circulation and Mixing Times [J]. Chem. Eng. Commun., 1982, 19(1): 141–147.